# Flow effects on multifragmentation in the canonical model

S. K. Samaddar,[1] J. N. De,[1,2,3] and S. Shlomo[3]
[1]*Saha Institute of Nuclear Physics, 1/AF Bidhannagar, Kolkata 700064, India*
[2]*Variable Energy Cyclotron Center, 1/AF Bidhannagar, Kolkata 700064, India*
[3]*The Cyclotron Institute, Texas A&M University, College Station, Texas 77843, USA*
(Received 14 November 2003; published 24 June 2004)

A prescription to incorporate the effects of nuclear flow on the process of multifragmentation of hot nuclei is proposed in an analytically solvable canonical model. Flow is simulated by the action of an effective negative external pressure. It favors sharpening the signatures of liquid-gas phase transition in finite nuclei with increased multiplicity and a lowered phase transition temperature.

DOI: 10.1103/PhysRevC.69.064615 PACS number(s): 24.10.Pa, 25.70.−z

In intermediate energy heavy ion reactions, particularly for the central and near-central collisions, the colliding nuclei get compressed in the initial phase with subsequent decompression thereby generating collective flow energy. At energies around 100 MeV per nucleon or above, large radial collective flow has been observed in many experiments [1–4]. Theoretically it has been surmised that collective expansion has a strong influence on the fragment multiplicity. In a hydrodynamical model with site-bond percolation, it has been shown that compression is very effective [5] in multifragmentation. Such a conclusion is further reached in microscopic BUU-type formulations [6] as well as in a grand canonical thermodynamic calculation [7]. Its crucial importance on the extracted value of the freeze-out density from yield ratios of fragment isotopes differing by one neutron [8,9] in a statistical fragmentation model was also pointed out [10].

Speculations have been made connecting multifragmentation to a liquid-gas type phase transition in finite nuclear systems (detailed references may be found in Refs. [11–13]). Experimental determination of the caloric curves in nuclear multifragmentation studies suggest strongly the occurrence of such a transition. The determination of temperature, however, is still shrouded in uncertainty and the order of the transition is a subject of controversy. Theoretical models of different genres have been proposed; these include percolation [14], lattice-gas [15,16], statistical canonical [11] and microcanonical models [12] and semimicroscopic models like finite temperature Thomas-Fermi theory in both nonrelativistic [17] and relativistic [18] framework. Many of these models are based on the phase space considerations though they differ in details. A canonical model based on this consideration which is analytic in nature has been proposed in Ref. [19] and some applications [20,21] of this model have been made in the context of nuclear mutifragmentation. This model is comparatively easily tractable, but still powerful enough to reproduce many of the features of nuclear multifragmentation including liquid-gas phase transition that can be correlated to some of the experimental data. This model, however, does not include the effects of nuclear flow observed in intermediate energy heavy ion collisions. In this communication we incorporate nuclear flow in the model and study its effect on some inclusive multifragmentation observables.

The flow effects are simulated through an external negative pressure [7]. In the stationary freeze-out volume calculation as no nucleonic matter exists beyond the freeze-out boundary, the external pressure is assumed to be zero. A positive uniform external pressure, i.e., an inwardly directed pressure, gives rise to compression of the system. Similarly, a negative external pressure gives rise to an inflationary scenario (as in the case of early universe [22], for example). The expanding nuclear system can then be simulated as under the action of an effective negative external pressure. We define the flow pressure to be equal and opposite to this negative external pressure. It should be pointed out that the validity of the model depends on the assumption that the thermodynamic equilibration time is small compared to the time scale for the expansion of the system. This is expected to be fulfilled [7] when $v_{\mathrm{flow}}/\langle v\rangle$ is much small compared to unity; here $\langle v\rangle$ is the average nucleonic velocity. This limits the applicability of the model to flow energy up to $\sim$5 MeV per nucleon.

We consider an excited nuclear system at a temperature $T$ and under an external pressure $P$ (negative in our case, the flow pressure $P_{\mathrm{fl}}=-P$). The system consists of $N$ neutrons and $Z$ protons, the total number of nucleons being $A(=N+Z)$. The partition function $Q_{A,Z}$ of the system [23] is given by

$$Q_{A,Z}=\exp(-G/T)=\sum_{r}\exp[-(E_r+PV_r)/T]. \qquad (1)$$

Here $G=E-TS+PV$ is the Gibbs potential, $E_r$ the state dependent energy and $V_r$ the state dependent volume. If $\omega_{ij}$ represents the partition function for the fragment $(ij)$ consisting of $i$ nucleons and $j$ protons, the partition function of the system $(A,Z)$ fragmenting into all possible configurations $\{\mathbf{n}\}$, assuming the fragment pieces are noninteracting, is given by

$$Q_{A,Z}=\sum_{\{\mathbf{n}\}}\prod_{i=1}^{A}\prod_{j=0}^{Z}\frac{(\omega_{ij})^{n_{ij}}}{n_{ij}!}. \qquad (2)$$

Here $n_{ij}$ is the number of $(ij)$ species present. The sum runs over all possible configurations conserving nucleon number and charge. The average multiplicity of $(ij)$ species is

 

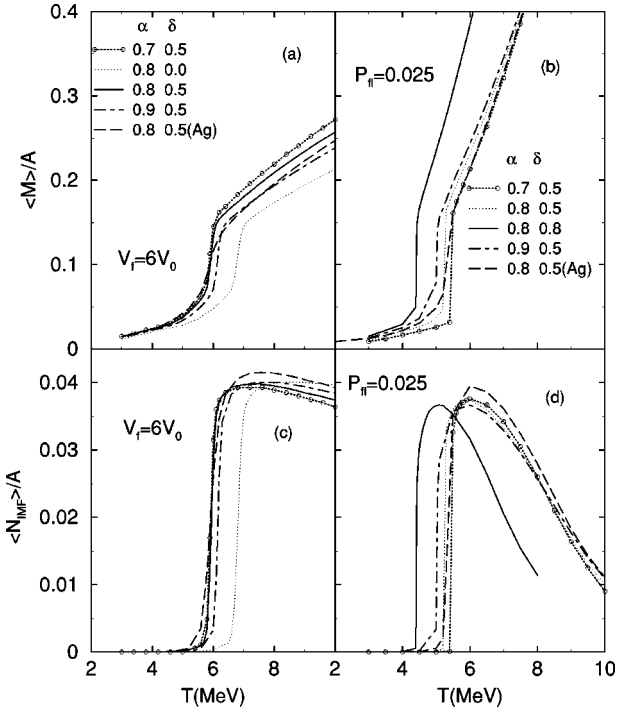


FIG. 1. In the top panel the average multiplicities per nucleon $\langle M\rangle/A$ as a function of temperature at constant volume (a) and at constant flow pressure $P_{\rm fl}=0.025$ MeV fm$^{-3}$ (b) are shown. All lines correspond to $^{197}$Au except the dashed line that refers to $^{109}$Ag. The different lines refer to different sets of flow parameters as given in the legend. In the bottom panel the average IMF multiplicity per nucleon $\langle N_{\rm IMF}\rangle/A$ is displayed both at constant volume (c) and at constant flow pressure (d). The notations for the panels (c) and (d) are the same as those in the panels (a) and (b), respectively.

$$\langle n_{ij}\rangle = \frac{\omega_{ij}}{Q_{A,Z}} Q_{A-i,Z-j}. \tag{3}$$

The function $Q_{A,Z}$ can be easily calculated using the recursion relation [19]

$$Q_{A,Z} = \frac{1}{A}\sum_{i=1}^{A}\sum_{j=0}^{Z} i\omega_{ij} Q_{A-i,Z-j}. \tag{4}$$

The partition function is built up defining $Q_{00}=1$. The partition function $\omega_{ij}$ is

$$\omega_{ij} = \sum_k \int \frac{d^3p\, d^3r}{h^3} \exp\left[-\left(E_{ij}^k + \frac{P_{ij}V}{n_{ij}}\right)\Big/ T\right], \tag{5}$$

where $P_{ij}(\Sigma_{ij} P_{ij}=P)$ is the partial pressure due to the $(ij)$ species and

$$E_{ij}^k = \frac{p^2}{2mi} + \epsilon_{ij}^k + V_{ij}^C. \tag{6}$$

Here the first term on the right-hand side denotes the center of mass kinetic energy and $\epsilon_{ij}^k$ refers to the energy of the $k$th internal state of the fragment; $V_{ij}^C$ is the single-particle Coulomb energy which we evaluate in the complementary fragment approximation [24]. Equation (5) reduces to

$$\omega_{ij} = \frac{(2\pi mT)^{3/2}}{h^3} i^{3/2} q_{ij} \int dV \exp(-P_{ij}V/n_{ij}T), \tag{7}$$

where

$$q_{ij} = \sum_k \exp[-(\epsilon_{ij}^k + V_{ij}^C)/T]. \tag{8}$$

We do not have any *a priori* notion about the dependence of $P_{ij}$ and $n_{ij}$ on volume as well as on temperature. We, therefore, make a simplifying assumption that the dependence of $P_{ij}V/n_{ij}=P_{ij}/\rho_{ij}$ [$\rho_{ij}$ being the density of the $(ij)$ species] on temperature is linear. It will be seen later that this is tantamount to assuming the flow energy of a fragment proportional to temperature. Such a prescription may not be unjustified as both stronger compression (hence collective flow) and larger temperature of the fragmenting system result from enhanced bombarding energy. We then write $P_{ij}/\rho_{ij}=C_{ij}T$, $C_{ij}$ being a constant for the fragment species.

For fragment masses up to $i=16$, the input for $\epsilon_{ij}^k$ is taken from the experimental data; for fragment masses above 16, the liquid-drop expression

$$q_{ij} = \exp[(W_0 i - \sigma(T) i^{2/3} + a_i T^2 - V_{ij}^C)/T], \tag{9}$$

is taken using Fermi-gas approximation. Here the volume energy term $W_0=16$ MeV, the temperature dependent surface tension is $\sigma(T)=\sigma_0[(T_c^2-T^2)/(T_c^2+T^2)]^{5/4}$ with $\sigma_0=18$ MeV, and the critical temperature $T_c=18$ MeV. The level density parameter is taken as $a_i=i/16$ MeV$^{-1}$.

The total energy of the system is evaluated as

$$\begin{aligned} E &= \frac{1}{Q_{A,Z}}\sum_r E_r \exp[-(E_r + PV_r)/T] \\ &= \sum_{ij}\langle n_{ij}\rangle\left[\frac{3}{2}T + \left\{ i(-W_0 + T^2/16) + \sigma(T) i^{2/3} \right.\right. \\ &\quad \left.\left. - T\frac{d\sigma}{dT} i^{2/3} + V_{ij}^C \right\}\right] - P\langle V\rangle. \end{aligned} \tag{10}$$

In deriving Eq. (10), use has been made of the same approximation as in Eq. (7). The first term in the square brackets is the kinetic energy of the fragments for the center of mass motion and the term within the curly bracket is the internal energy of the fragments lifted by the Coulomb energy. The last term is identified as the flow energy (note here that $P$ is negative). In absence of a better prescription, we have replaced the average volume $\langle V\rangle$ by a freeze-out volume $V_f$. It is then seen that the flow energy $e_{\rm fl}^{ij}$ of a fragment belonging to the $(ij)$ species is $P_{ij}/\rho_{ij}$. We then have $e_{\rm fl}^{ij}=C_{ij}T$. We consider the flow to be radial. As the heavier fragments are formed relatively closer to the center, the flow energy per particle decreases with the mass number of the fragment. So we parametrize $e_{\rm fl}^{ij}$ as $\delta i^{\alpha} T$ with $\alpha<1$. The parameter $\delta$ determines the flow energy of a nucleon at a temperature $T$. The total flow energy is

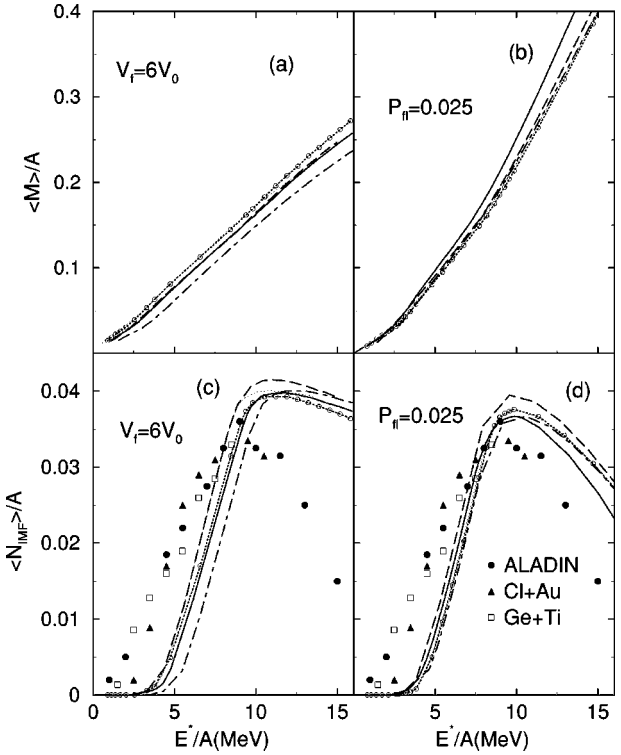


FIG. 2. The average multiplicity per nucleon $\langle M\rangle/A$ (top panel) and the average IMF multiplicity per nucleon $\langle N_{\mathrm{IMF}}\rangle/A$ (bottom panel) are shown as a function of excitation energy. The notations are the same as in Fig. 1. Some representative experimental data for IMF multiplicity are also displayed.

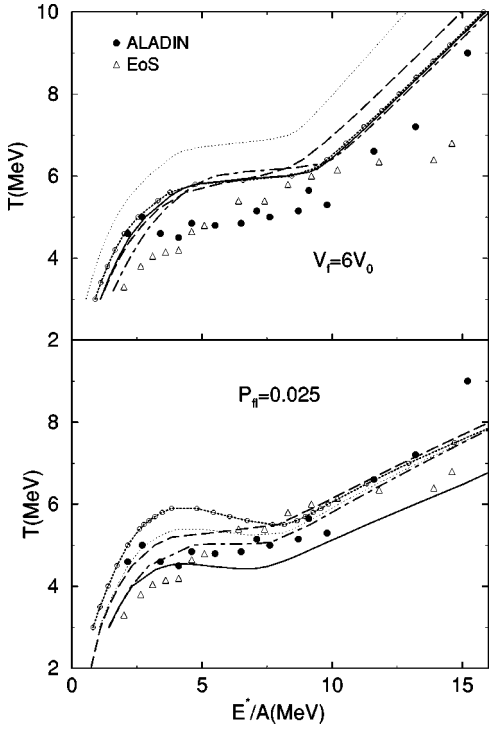


FIG. 3. The caloric curves at constant freeze-out volume $V_f = 6V_0$ (top panel) and at constant flow pressure $P_{\mathrm{fl}} = 0.025$ MeV fm$^{-3}$ (bottom panel). The notations are the same as in Fig. 1. The experimental data refer to Refs. [4] (filled circles) and [25] (open triangles).

$$E_{\mathrm{fl}}^{\mathrm{tot}} = \delta T \sum_{ij} \langle n_{ij}\rangle i^{\alpha}. \tag{11}$$

The decrease of flow energy per particle with increasing mass of the fragment is taken care of through the parameter $\alpha$. It can be checked that for $\alpha=1$, the fragmentation pattern remains unaltered. With these prescriptions, the integral pertaining to Eq. (7) is $V_f \exp(\delta i^{\alpha})$. The effect of flow is thus tantamount to an increase in the effective freeze-out volume which is dependent on the fragment species. The larger the species, the larger the effective freeze-out volume. Such an effect was already observed in a previous analysis of experimental data with radial flow [10].

In order to study the flow effects on nuclear multifragmentation, results are shown for $^{197}$Au taken as a representative system along with those for $^{109}$Ag to explore the mass dependence of the observables calculated. An *ab initio* determination of the parameters $\alpha$ and $\delta$ is beyond the scope of a statistical model. We vary the parameters $\alpha$ and $\delta$ to study their sensitivity on the observables. In Fig. 1, the average per nucleon multiplicity $\langle M\rangle/A$ (top panels) and the average number of intermediate mass fragments per nucleon $\langle N_{\mathrm{IMF}}\rangle/A$ (bottom panels) are displayed as a function of temperature. The IMF's are defined as fragments with $3 \leqslant Z \leqslant 20$. In panel (a) the fragment multiplicities that are displayed are calculated at a constant freeze-out volume $V_f = 6V_0$ where $V_0$ is the normal volume of the fragmenting system. All the subsequent calculations at constant volume are done at the aforementioned $V_f$. The meanings of the different lines corresponding to variation of $\alpha$ and $\delta$ are displayed in the legend. Unless specifically mentioned in the legend, the lines correspond to $^{197}$Au as the fragmenting system. The comparison of the dotted line with the full line shows the influence of flow on the fragment multiplicity. It is evident that flow enhances the multiplicity. We note that the multiplicity $\langle M\rangle/A$ has a sudden enhancement at a particular temperature. It will be seen later that such enhancement also occurs in the heat capacity and entropy at around this temperature which we identify as a liquid-gas type phase transition in a finite nucleus. This transition temperature decreases with increasing flow. At a constant volume, we note that generally multiplicity increases with decreasing $\alpha$. The multiplicity and the transition temperature are weakly dependent on the parameter $\alpha$. Their dependence on the mass of the fragmenting system is also not very significant as is evident from the results displayed for $^{109}$Ag (dashed line) in the figure. The fragment multiplicity at constant flow pressure $P_{\mathrm{fl}} = 0.025$ MeV fm$^{-3}$ is displayed in the panel (b). The values of the parameter sets corresponding to different lines are given in the legend. For all the results presented in Figs. 1–3, the legends of panels (a) and (b) apply for calculations performed at constant volume and at constant flow pressure, respectively. From the comparison of the solid line and the dotted line it is found that the multiplicity increases significantly with the increase in the flow energy. As in the case of constant volume, the multiplicity is seen to be not sensitive

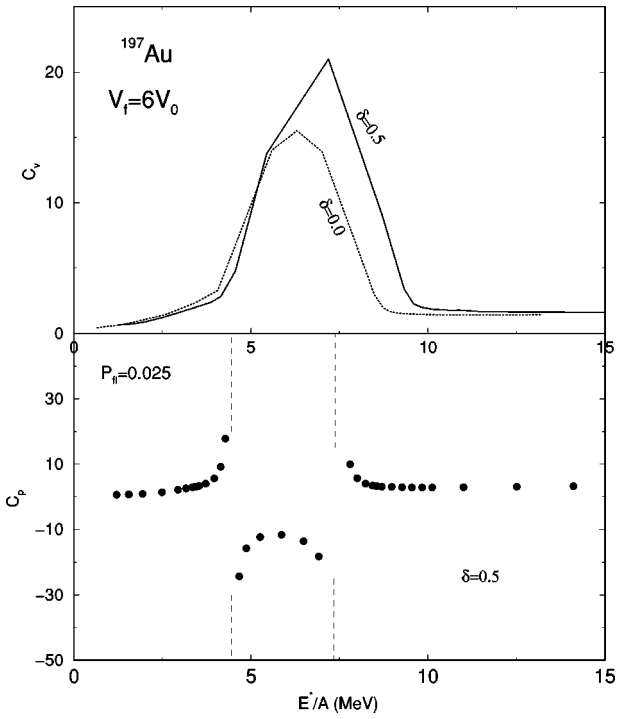


FIG. 4. The heat capacity per nucleon at constant volume $6V_0$ (top panel) and at constant flow pressure 0.025 MeV fm$^{-3}$ (bottom panel) are displayed for $^{197}$Au with $\alpha=0.8$ and $\delta$ as indicated. The meaning of the vertical dashed lines is explained in the text.

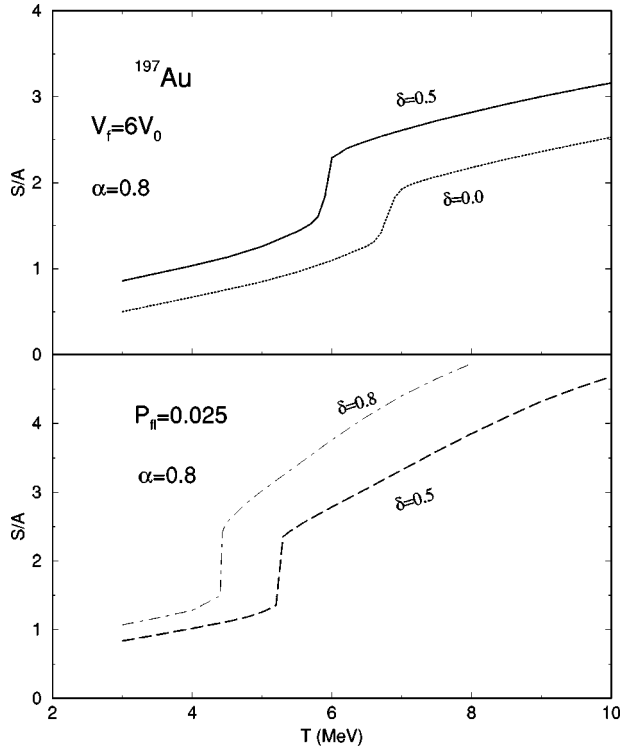


FIG. 5. The entropy per nucleon $S/A$ at constant volume $6V_0$ (top panel) and at constant flow pressure 0.025 MeV fm$^{-3}$ (bottom panel) with $\alpha$ and $\delta$ as indicated for the system $^{197}$Au.

to the parameter $\alpha$ and the mass of the fragmenting system. The jump at the transition temperature is somewhat more marked here as compared to that for constant volume calculations. The total flow energy is quite insensitive to the parameter $\alpha$ and is mostly governed by the parameter $\delta$. For $\delta=0.5$, at the transition temperature the flow energy is $\sim$1.6 MeV per nucleon which increases to $\sim$2.3 MeV per nucleon for $\delta=0.8$. In the lower panels of the figure, the average number of intermediate mass fragments per nucleon $\langle N_{\mathrm{IMF}}\rangle/A$ are displayed as a function of temperature both at constant volume and at constant flow pressure as indicated. Below the transition temperature the number of $N_{\mathrm{IMF}}$'s are very small; at the transition temperature there is a sudden enhancement in the IMF multiplicity. The dependence of $\langle N_{\mathrm{IMF}}\rangle/A$ on the parameters $\alpha$ and $\delta$ as well as on the mass of the fragmenting system are similar as found for the fragment multiplicity $\langle M\rangle/A$.

Experimentally, the multiplicities are measured as a function of excitation energy. The calculated results along with the measured $\langle N_{\mathrm{IMF}}\rangle/A$ as a function of $E^*/A$ both at constant volume and at constant pressure are displayed in Fig. 2. The average multiplicity per nucleon $\langle M\rangle/A$ is seen to increase smoothly with $E^*/A$; the $\langle N_{\mathrm{IMF}}\rangle/A$ is found to rise and fall smoothly as a function of excitation energy. It is found that the calculated results at constant pressure conforms better with the experimental data. In the experimental situation, the mass of the fragmenting system decreases appreciably with the excitation energy. However, from the calculated results for Ag and Au, we find that the IMF multiplicities nicely scale with the mass of the fragmenting system. This justifies the comparison of $\langle N_{\mathrm{IMF}}\rangle/A$ calculated for a single system for all the excitation energies with the experimental data.

The caloric curves, i.e., the dependence of the excitation energy on temperature both at constant volume (top panel) and at constant pressure (bottom panel) are presented in Fig. 3. The dashed line corresponds to $^{109}$Ag, the other ones refer to Au with different choices of parameters as explained in connection with Fig. 1. The caloric curve at constant volume shows a monotonic increase of temperature with excitation energy; however, a clear plateau is observed at around $T=6.7$ MeV for calculation without flow and at $\sim$5.8 MeV for all values of $\alpha$ chosen with $\delta=0.5$. A few representative experimental data (given by filled circles [4] and open triangles [25]) are shown in the figure. There is a wide variation in mass of the excited fragmenting system in these data. Mass variation is an important factor that has been often emphasized [26] in any interpretation of the caloric curve; however, in the mass range 100–200, there is not much quantitative change in the experimental data [27]. This is also reflected in our calculations. It is seen that with a modest flow energy of $\sim$2 MeV per nucleon around the transition temperature, the qualitative features of the data can be fairly reproduced. The caloric curve at constant flow pressure, on the other hand, exhibits instead of a plateau a mild undulation in a very narrow region of temperature near the phase transition. The excitation energy is triple valued at a fixed temperature in this region. This corresponds to three different freeze-out volumes. (For Figs. 1 and 5, the relevant quantities are taken at the highest volume where $G$ is found to be the minimum.)

In a canonical model without flow, such a behavior has also been observed at constant thermal pressure by Das *et al.* [28]. Inspection of the caloric curves both at constant volume and at constant pressure shows that they are nearly insensitive to the values of $\alpha$ and the mass of the fragmenting systems chosen. However, increase in flow energy (increase in $\delta$) reduces the transition temperature.

The heat capacity at constant volume $C_v$ as a function of excitation energy is shown in the top panel of Fig. 4 for the system $^{197}$Au with $\alpha=0.8$ and values of $\delta$ as marked in the figure. The peaked structure in $C_v$ signals a liquid-gas phase transition, the peak becoming stronger with increasing flow. Results corresponding to the choice of other parameters are not shown as they yield very similar results. The heat capacity at constant flow pressure (bottom panel) with $\delta=0.5$ and $\alpha=0.8$ shows a negative branch in the excitation energy zone corresponding to the narrow temperature range where the caloric curve displays a negative slope in the undulating region. The dashed vertical lines correspond to the maximum and minimum in the caloric curve where $C_p$ is discontinuous. Similar behavior has also been observed in the lattice-gas model by Chomaz *et al.* [16]. The qualitative nature of $C_p$ with choice of other flow parameters remains unchanged and are not shown.

The entropy per particle $S/A$ as a function of temperature at constant volume and at constant flow pressure $P_{\rm fl}$ are displayed in the top and in the bottom panel of Fig. 5, respectively, for the values of the flow parameters as given in the figure. At the transition temperature, there is a jump in the entropy which becomes more pronounced for calculations at constant $P_{\rm fl}$. The larger entropy at any particular temperature with flow can be understood either from the enhanced fragment multiplicity with flow or from the increased effective freeze-out volume.

In summary, we have performed calculations for multifragmentation of a heated nucleus in a canonical model with incorporation of flow both at constant volume as well as at constant flow pressure. It may be pointed out that under the experimental conditions none of these constraints may exist. In the absence of any definite knowledge of the actual scenario, the calculations are done with these constraints imposed. It is found that the average multiplicity increases with flow; the average IMF multiplicity shows a rise and fall with excitations commensurate with the experimental data. The calculated caloric curves also follow the experimental trend very closely. The plateau in the caloric curve and the peaked structure of the corresponding heat capacity at around 5–6 MeV signal a liquid-gas phase transition in the finite nuclear systems. At constant flow pressure, the caloric curve shows a negative slope in a small domain of temperature and gives rise to negative heat capacity. Negative heat capacity at constant thermal pressure has been observed in the same model without flow [28]; it is interpreted as arising in regions of mechanical instability where the isobaric volume expansion coefficient is negative. The same effect is seen to persist with incorporation of flow. A sudden jump in entropy is also seen, both at constant volume and at constant pressure. It is interesting to note that the maximum in the $\langle N_{\rm IMF}\rangle$, the peak in $C_v$, the discontinuity in $C_p$, and the sudden jump in entropy are all around the same temperature signalling a liquid-gas phase transition.

This work was supported in part by the U.S. Department of Energy under Grant No. FG03-93ER40773 and by the National Science Foundation under Grant No. NSF-0355200. J.N.D. gratefully acknowledges the warm hospitality at the Cyclotron Institute, Texas A&M University. S.K.S. is very thankful to the Council of Scientific and Industrial Research of the Government of India, for the financial support.

[1] S. C. Jeong *et al.*, Phys. Rev. Lett. **72**, 3468 (1994).
[2] W. C. Hsi *et al.*, Phys. Rev. Lett. **73**, 3367 (1994).
[3] G. J. Kunde *et al.*, Phys. Rev. Lett. **74**, 38 (1995).
[4] J. Pochodzalla *et al.*, Phys. Rev. Lett. **75**, 1040 (1995).
[5] J. Desbois, R. Boisgard, C. Ngo, and J. Nemeth, Z. Phys. A **328**, 101 (1987).
[6] H. M. Xu, C. A. Gagliardi, R. E. Tribble, and C. Y. Wong, Nucl. Phys. **A569**, 575 (1994).
[7] Subrata Pal, S. K. Samaddar, and J. N. De, Nucl. Phys. **A608**, 49 (1996).
[8] S. Albergo, S. Costa, E. Costanzo, and A. Rubbino, Nuovo Cimento Soc. Ital. Fis., A **A89**, 1 (1985).
[9] X. Campi, H. Krivine, and E. Plagnol, Phys. Lett. B **385**, 1 (1996).
[10] S. Shlomo, J. N. De, and A. Kolomiets, Phys. Rev. C **55**, R2155 (1997).
[11] J. P. Bondorf, A. S. Botvina, A. S. Iljinov, I. N. Mishustin, and K. Sneppen, Phys. Rep. **257**, 130 (1995).
[12] D. H. E. Gross, Phys. Rep. **279**, 119 (1997).
[13] B. Borderie, J. Phys. G **28**, R217 (2002).
[14] X. Campi, Phys. Lett. B **208**, 351 (1988).
[15] J. Pan and S. Dasgupta, Phys. Rev. C **57**, 1839 (1998).
[16] P. Chomaz, B. Duflot, and F. Gulminelli, Phys. Rev. Lett. **85**, 3587 (2000).
[17] J. N. De, S. Dasgupta, S. Shlomo, and S. K. Samaddar, Phys. Rev. C **55**, R1641 (1997).
[18] T. Sil, B. K. Agrawal, J. N. De, and S. K. Samaddar, Phys. Rev. C **63**, 054604 (2001).
[19] K. C. Chase and A. Z. Mekjian, Phys. Rev. C **50**, 2078 (1994).
[20] P. Bhattacharya, S. Dasgupta, and A. Z. Mekjian, Phys. Rev. C **60**, 064625 (1999).
[21] M. B. Tsang *et al.*, Phys. Rev. C **64**, 054615 (2001).
[22] A. H. Guth, Phys. Rev. D **23**, 347 (1981).
[23] S. K. Ma, *Statistical Mechanics* (World Scientific, Singapore, 1993), p. 106.
[24] D. H. E. Gross, L. Satpathy, M. T. Chung, and M. Satpathy, Z. Phys. A **309**, 41 (1982).
[25] J. A. Hauger *et al.*, Phys. Rev. Lett. **77**, 235 (1996).
[26] J. B. Natowitz *et al.*, Phys. Rev. C **52**, R2322 (1995).
[27] J. B. Natowitz *et al.*, Phys. Rev. C **65**, 034618 (2002).
[28] C. B. Das, S. Dasgupta, and A. Z. Mekjian, Phys. Rev. C **68**, 014607 (2003).